Karlsruher Institut für Technologie

Two-loop master integrals and form-factors for pseudo-scalar quarkonia

Melih A. Ozcelik

Institute for Theoretical Particle Physics, Karlsruhe Institute of Technology

melih.oezcelik@kit.edu

Collaborators: S. Abreu, M. Becchetti, C. Duhr

Loops & Legs 2022, Ettal,
27 April 2022

Outline

Introduction

Part I: Quarkonium phenomenology at NLO

Part II: Two-loop master integrals and form-factors

Part III: Decay of para-Positronium to di-photon at NNLO accuracy

Introduction: What is a Quarkonium?

- similar to positronium bound state $\mathrm{e}^+\mathrm{e}^-$ in QED
- bound state of heavy quark and its anti-quark in QCD, e.g. Charmonium (charm quark) and Bottomonium (bottom quark)

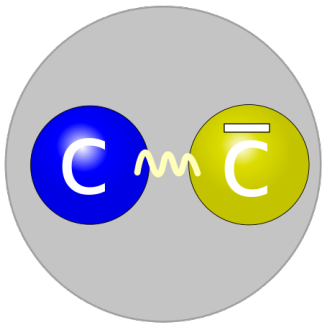

[Figure from Wikipedia 'Quarkonium']

- Toponium ($t\bar{t}$) bound state: high mass of top quark $\rightarrow$ decays via weak interaction before formation of bound state
- for light quarks: mixing between (u,d,s) quarks due to low mass difference $\rightarrow$ π-meson, the ρ-meson and the η-meson

Motivation: Why study Quarkonia?

- charmonium production allows us to probe QCD at its interplay between the perturbative and non-perturbative regimes
- deeper understanding of confinement (production mechanism)
- access to spin/momentum distribution of gluons in protons
  $\rightarrow$ use quarkonia to constrain the gluon PDFs in the proton
- it is interesting to assess the convergence of perturbative expansion in α_s where $\alpha_s(m_c) \sim 0.34$ and $\alpha_s(m_b) \sim 0.22$

Part I

Quarkonium phenomenology at NLO

based on arXiv:1907.01400 and arXiv:2012.00702

the η_c - a good gluon probe

- η_c is a gluon probe at low scales at $M_{\eta_c} = 3$ GeV
- is a pseudo-scalar particle and simplest of all quarkonia as far as computation of hadro-production
- η_c cross section computation known
  - at NLO since 1992 in collinear factorisation

    [J. Kühn, E. Mirkes, Phys.Lett. B296 (1992) 425-429]
  - at LO since 2012 and at NLO since 2013 in TMD factorisation

    [D. Boer, C. Pisano, Phys.Rev. D86 (2012) 094007]

    [J.P. Ma, J.X. Wang, S. Zhao, Phys.Rev. D88 (2013) no.1, 014027]

problem of negative cross-sections - η_c and J/ψ at NLO

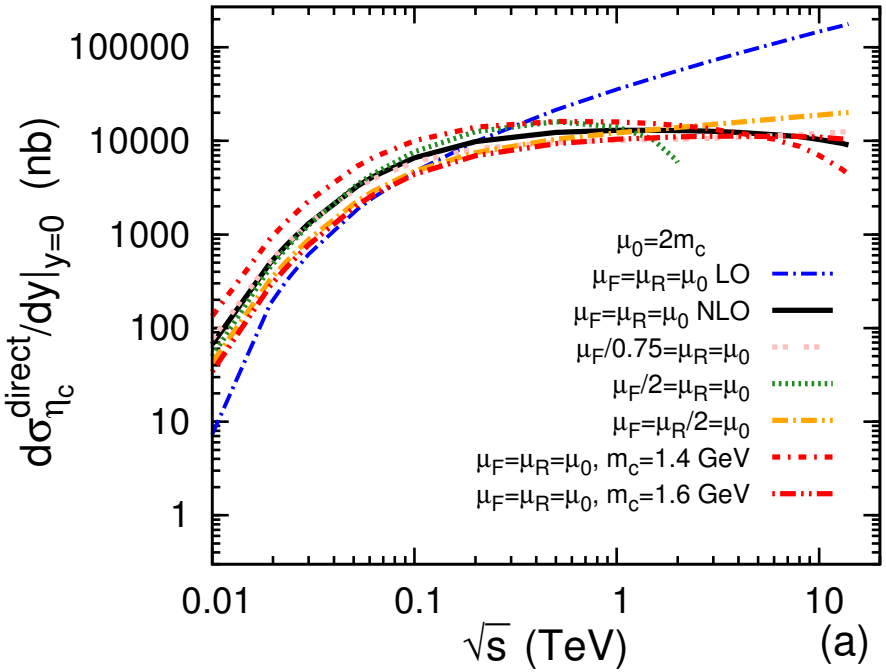

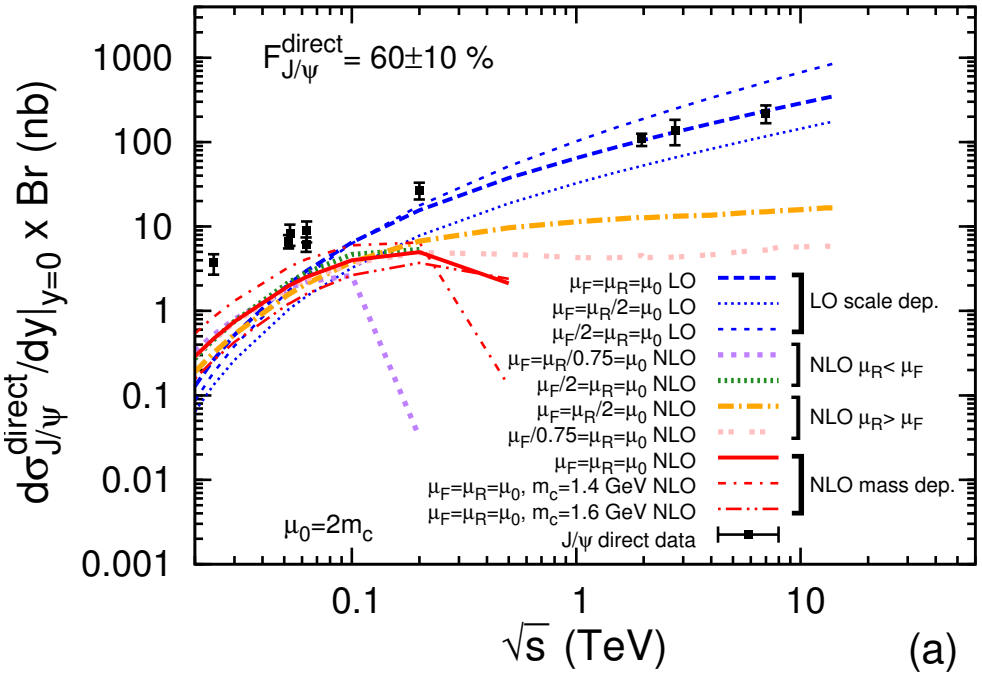

comparison of η_c (left) and J/ψ (right) differential cross-sections at NLO with different scale choices of μ_R and μ_F with CTEQ6M

[Y. Feng, J.-P. Lansberg, J.X. Wang, Eur.Phys.J. C75 (2015) no.7, 313]

partonic high-energy limit

Definition

$$\lim_{\hat{s}\to\infty} \hat{\sigma}_{ab}^{\mathrm{NLO}}(\hat{s}) = C_{ab}\frac{\alpha_s}{\pi}\hat{\sigma}_0^{\mathrm{LO}}\left(\log\frac{M_Q^2}{\mu_F^2} + \hat{A}\right) \tag{1}$$

- for ${}^1S_0^{[1,8]}$: $\boxed{\hat{A} = A_{gg} = A_{qg} = -1}$
- for $\mu_F = M_Q$, this limit is negative $\rightarrow$ $\propto -\frac{\alpha_s}{\pi}\hat{\sigma}_0^{\mathrm{LO}}$
- limit is most dominant contribution for flat gluon PDFs at low x $\rightarrow$ negative hadronic cross-section

a new scale prescription for μ_F

- We have mismatch because $\hat{A}$ is *process-dependent* while DGLAP evolution is *process-independent*.
- Keeping this in mind, we propose a new scale prescription for μ_F,

[J.-P. Lansberg, Melih A. Ozcelik, Eur.Phys.J.C 81 (2021) 6, 497 (arXiv:2012.00702)]

$$\boxed{\mu_F = \hat{\mu}_F = M e^{\hat{A}/2}}$$

such that $\left(\log \frac{M_Q^2}{\mu_F^2} + \hat{A}\right) = 0 \quad \rightarrow \quad \lim_{z\to 0} \hat{\sigma}_{ab}^{\mathrm{NLO}}(z) = 0.$

- scale choice for η_Q are within typical bounds $[\frac{M}{2}, 2M]$

$\frac{d\sigma}{dy}$ K-factor for η_c-production at $y = 0$

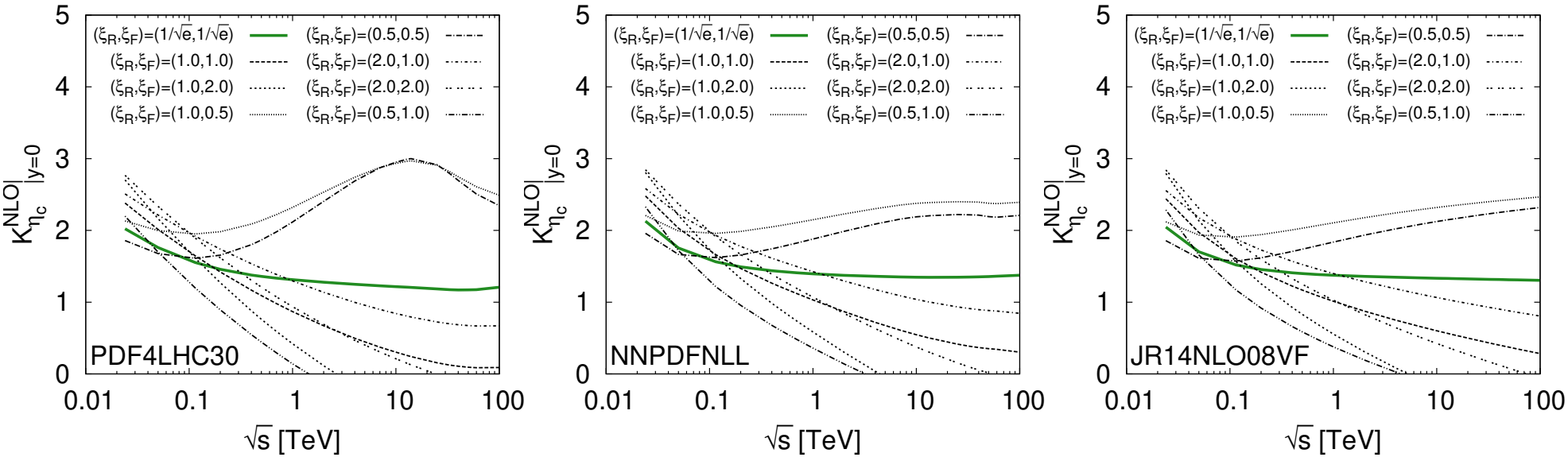

- K-factor: assess perturbative convergence
- **new scale choice** $\hat{\mu}_F$ (green curve) ✓:
  - perturbatively stable over energy range ✓
  - very similar results with different PDF parametrisation ✓
- other μ_F scale choices:
  - not perturbative stable and negative results at large energy ✗
  - different results with different PDF parametrisation ✗

Part I: Prospects

- used new scale prescription $\hat{\mu}_F$ to cure negative numbers for η_c hadro-production and J/ψ photo-production

[J.-P. Lansberg, Melih A. Ozcelik, Eur.Phys.J.C 81 (2021) 6, 497 (arXiv:2012.00702)]

[A. C. Serri, C. Flore, J.-P. Lansberg, Melih A. Ozcelik, H. S. Shao, Y. Yedelkina, arXiv:2112.05060]

- confirmed connection to high-energy factorisation

[J.-P. Lansberg, M. Nefedov, Melih A. Ozcelik, arXiv:2112.06789]

- prospect of including charmonium data in global PDF fits to constrain gluon PDFs at low scales

- for reduction of scale uncertainties need to go to NNLO level
  $\rightarrow$ need to compute two-loop master integrals with massive propagators

Part II

Two-loop master integrals and form-factors

Form-factors

- compute two-loop form-factors analytically in different channels that contribute at NNLO accuracy
  - $\gamma\gamma \leftrightarrow \eta_Q \left({}^1S_0^{[1]} \right) \rightarrow$ exclusive/inclusive decay
  - $gg \leftrightarrow \eta_Q \left({}^1S_0^{[1]} \right) \rightarrow$ **hadro-production** and hadronic decay width
  - $\gamma g \leftrightarrow {}^1S_0^{[8]} \rightarrow$ colour-octet contribution
  - $gg \leftrightarrow {}^1S_0^{[8]} \rightarrow$ colour-octet contribution
  - $\gamma\gamma \leftrightarrow$ para-Positronium

Form-factors

- compute two-loop form-factors analytically in different channels that contribute at NNLO accuracy
  - $\gamma\gamma \leftrightarrow \eta_Q \left({}^1S_0^{[1]} \right) \rightarrow$ exclusive/inclusive decay
  - $gg \leftrightarrow \eta_Q \left({}^1S_0^{[1]} \right) \rightarrow$ **hadro-production** and hadronic decay width
  - $\gamma g \leftrightarrow {}^1S_0^{[8]} \rightarrow$ colour-octet contribution
  - $gg \leftrightarrow {}^1S_0^{[8]} \rightarrow$ colour-octet contribution
  - $\gamma\gamma \leftrightarrow$ para-Positronium
- form-factors applicable to both production and decay

Form-factors

- compute two-loop form-factors analytically in different channels that contribute at NNLO accuracy
  - $\gamma\gamma \leftrightarrow \eta_Q \left({}^1S_0^{[1]} \right) \rightarrow$ exclusive/inclusive decay
  - $gg \leftrightarrow \eta_Q \left({}^1S_0^{[1]} \right) \rightarrow$ **hadro-production** and hadronic decay width
  - $\gamma g \leftrightarrow {}^1S_0^{[8]} \rightarrow$ colour-octet contribution
  - $gg \leftrightarrow {}^1S_0^{[8]} \rightarrow$ colour-octet contribution
  - $\gamma\gamma \leftrightarrow$ para-Positronium
- form-factors applicable to both production and decay
- in the past form-factors have been computed only in numerical form
  - $\eta_Q \rightarrow \gamma\gamma$ **[A. Czarnecki, K. Melnikov, Phys.Lett.B 519 (2001) 212-218] [F. Feng, Y. Jia, W.-L. Sang, Phys.Rev.Lett. 115 (2015) 22, 222001]**
  - para-Positronium $\rightarrow \gamma\gamma$ **[A. Czarnecki, K. Melnikov, A. Yelkhovsky, Phys.Rev.A 61 (2000) 052502]**

Amplitude generation & partial fraction

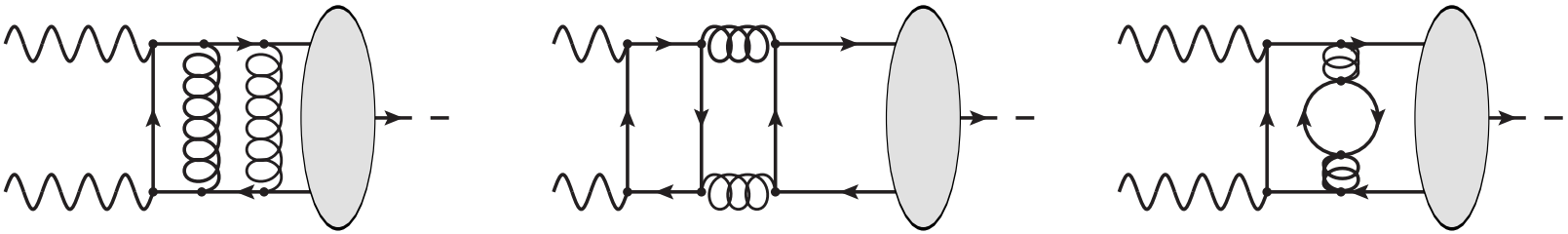

$$\gamma(k_1) + \gamma(k_2) \to Q(p_1)\overline{Q}(p_2) \tag{2}$$

Amplitude generation & partial fraction

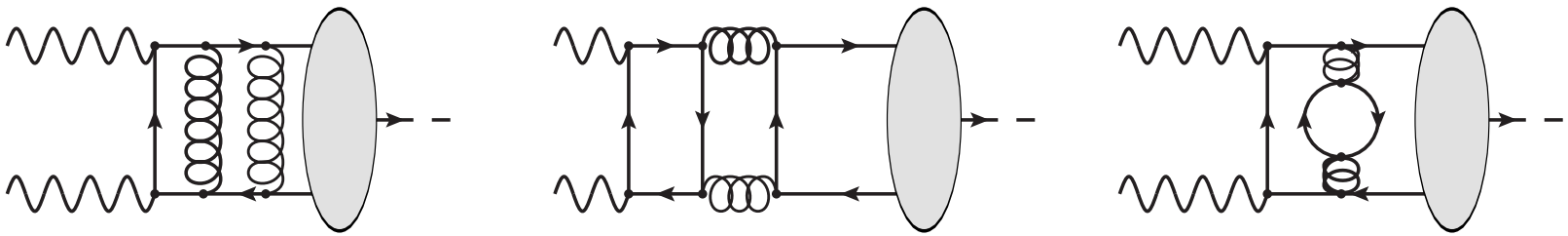

$$\gamma(k_1) + \gamma(k_2) \to Q(p_1)\overline{Q}(p_2) \tag{2}$$

- $p^2 = m_Q^2$ for final-state heavy quarks with $\boxed{p = p_1 = p_2}$
- $k_1^2 = k_2^2 = 0$ for initial-state photons
- threshold kinematics with $\boxed{\hat{s} = M_{\mathcal{Q}}^2 = 4m_Q^2}$ where $M_{\mathcal{Q}} = 2m_Q$

Amplitude generation & partial fraction

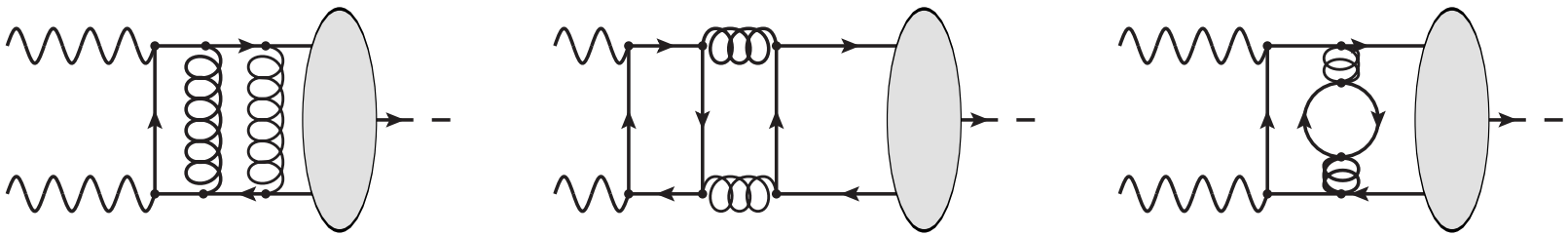

$$\gamma(k_1) + \gamma(k_2) \to Q(p_1)\overline{Q}(p_2) \tag{2}$$

- $p^2 = m_Q^2$ for final-state heavy quarks with $\boxed{p = p_1 = p_2}$
- $k_1^2 = k_2^2 = 0$ for initial-state photons
- threshold kinematics with $\boxed{\hat{s} = M_{\mathcal{Q}}^2 = 4m_Q^2}$ where $M_{\mathcal{Q}} = 2m_Q$

- generate Feynman diagram with `FeynArts` ($\sim$ 450 diagrams for $gg \leftrightarrow \eta_Q$ case)

Amplitude generation & partial fraction

The fact that the two heavy-quark momenta are equal allows us to simplify some integrals beforehand via the procedure of partial fractioning

Example

Feynman diagram:

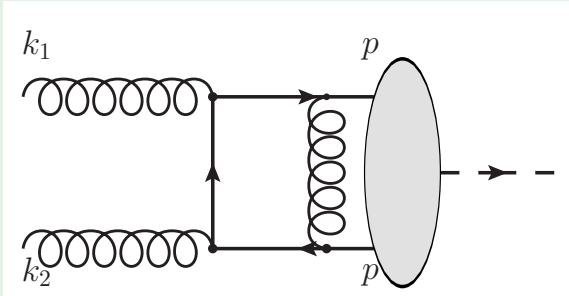

Amplitude generation & partial fraction

The fact that the two heavy-quark momenta are equal allows us to simplify some integrals beforehand via the procedure of partial fractioning

Example

Feynman diagram:

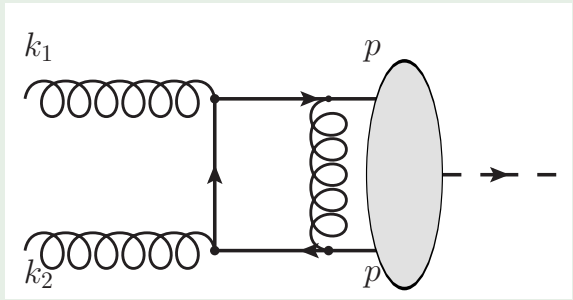

$$I_{\text{Coul.}} = \int d^D q_1 \frac{1}{D_1 D_2 D_3 D_4} = \tag{3}$$

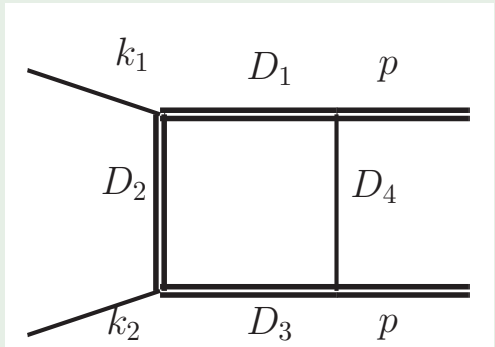

Amplitude generation & partial fraction

The fact that the two heavy-quark momenta are equal allows us to simplify some integrals beforehand via the procedure of partial fractioning

Example

Feynman diagram:

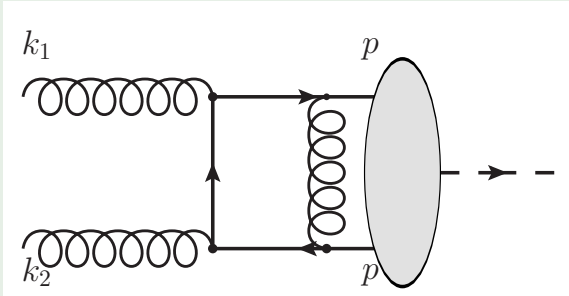

$$I_{\text{Coul.}} = \int d^D q_1 \frac{1}{D_1 D_2 D_3 D_4} = \tag{3}$$

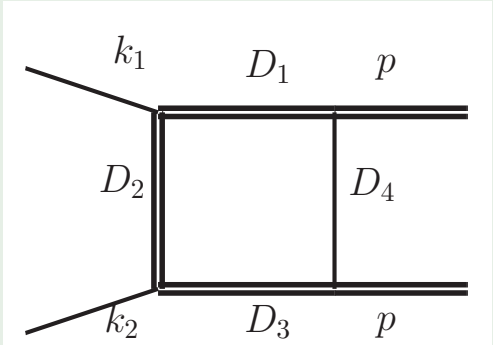

Denominators are linearly dependent: $D_4 = \frac{1}{2}(D_1 + D_3)$

Amplitude generation & partial fraction

Example

Feynman diagram:

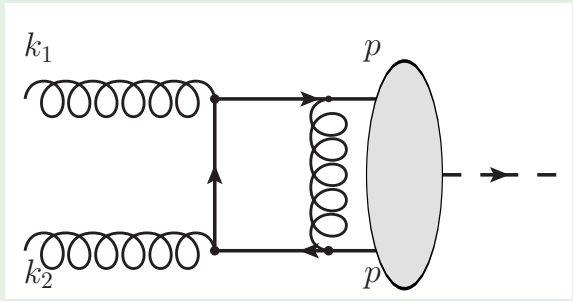

$$I_{\text{Coul.}} = \int d^D q_1 \frac{1}{D_1 D_2 D_3 D_4} = \int d^D q_1 \frac{2}{D_1 D_2 D_3^2} - \int d^D q_1 \frac{1}{D_2 D_3^2 D_4} \quad (4)$$

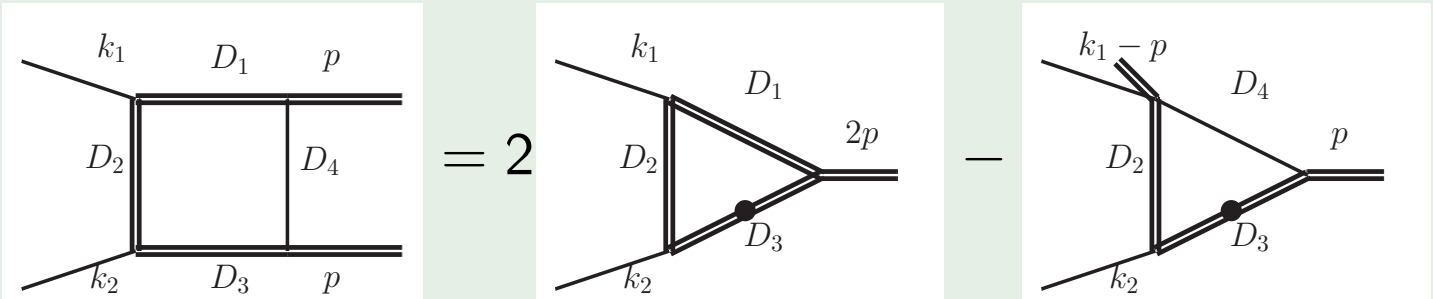

(5)

Amplitude generation & partial fraction

- partial fraction allows us to simplify integrals,
  4-point function $\rightarrow$ 3-point function

Amplitude generation & partial fraction

- partial fraction allows us to simplify integrals,
  4-point function $\rightarrow$ 3-point function

- at higher loop orders, many denominators are involved
  $\rightarrow$ linearly dependent denominators can be systematically detected

Amplitude generation & partial fraction

- partial fraction allows us to simplify integrals,
  4-point function $\rightarrow$ 3-point function
- at higher loop orders, many denominators are involved
  $\rightarrow$ linearly dependent denominators can be systematically detected
- partial fractioning can be performed with `$Apart`-package

[F. Feng, Comput.Phys.Commun. 183 (2012) 2158-2164]

Amplitude generation & partial fraction

- partial fraction allows us to simplify integrals,
  4-point function $\rightarrow$ 3-point function
- at higher loop orders, many denominators are involved
  $\rightarrow$ linearly dependent denominators can be systematically detected
- partial fractioning can be performed with `$Apart`-package

  [F. Feng, Comput.Phys.Commun. 183 (2012) 2158-2164]
- perform tensor integral decomposition in new basis

Amplitude generation & partial fraction

- partial fraction allows us to simplify integrals,
  4-point function $\rightarrow$ 3-point function
- at higher loop orders, many denominators are involved
  $\rightarrow$ linearly dependent denominators can be systematically detected
- partial fractioning can be performed with `$Apart`-package

  [F. Feng, Comput.Phys.Commun. 183 (2012) 2158-2164]
- perform tensor integral decomposition in new basis
- reduce integrals to master integrals via IBP with `FIRE`

  [A.V. Smirnov, Comput.Phys.Commun. 189 (2015) 182-191]

Amplitude

- two-loop Amplitude $\mathcal{A}^{(2)}$:

$$\mathcal{A}^{(2)} = \mathcal{A}^{(0)} \sum_{i=1}^{n_{\text{master}}} c_i(\epsilon)\text{MI}[i] \tag{6}$$

- tree-level Amplitude $\mathcal{A}^{(0)}$
- coefficient c_i contains information on:
  - rational factor depending on dimensional regulator ϵ
  - colour factor (C_A, C_F, T_F)
  - number of massive (n_h) and massless (n_l) closed fermion loops (vacuum & light-by-light)
- need to compute master integrals MI[i]

Topologies and master integrals

Some examples of topologies:

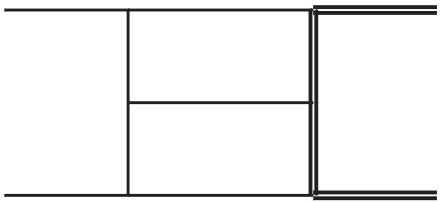

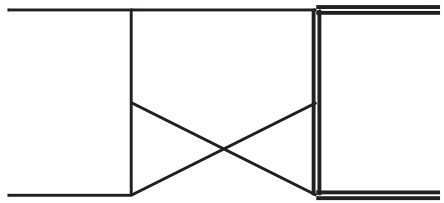

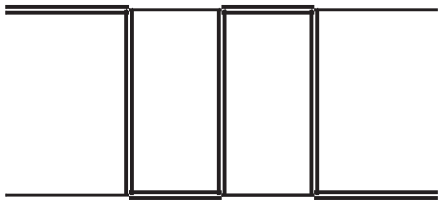

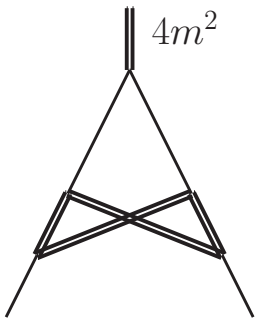

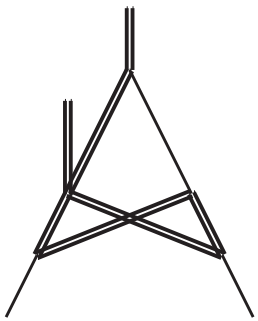

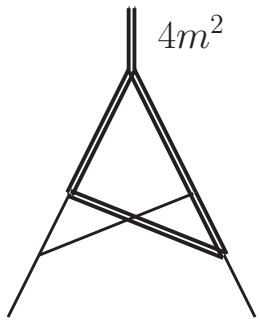

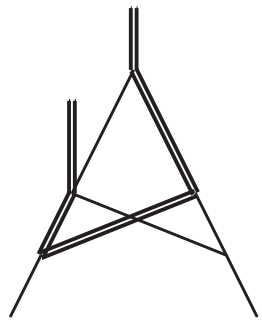

Topologies and master integrals

- Appearance of 76 master integrals in total

Topologies and master integrals

- Appearance of 76 master integrals in total
- some are known in general kinematics (see later) but not usable at special kinematics

Topologies and master integrals

- Appearance of 76 master integrals in total
- some are known in general kinematics (see later) but not usable at special kinematics
- Master integrals are seemingly independent, however we find some interesting equivalence relations beyond IBP

Topologies and master integrals

- Appearance of 76 master integrals in total
- some are known in general kinematics (see later) but not usable at special kinematics
- Master integrals are seemingly independent, however we find some interesting equivalence relations beyond IBP
  - **Partial Fraction Relations**

Topologies and master integrals

- Appearance of 76 master integrals in total
- some are known in general kinematics (see later) but not usable at special kinematics
- Master integrals are seemingly independent, however we find some interesting equivalence relations beyond IBP
  - **Partial Fraction Relations**
  - **Triangle Relations**

Partial Fraction Identities

Identity

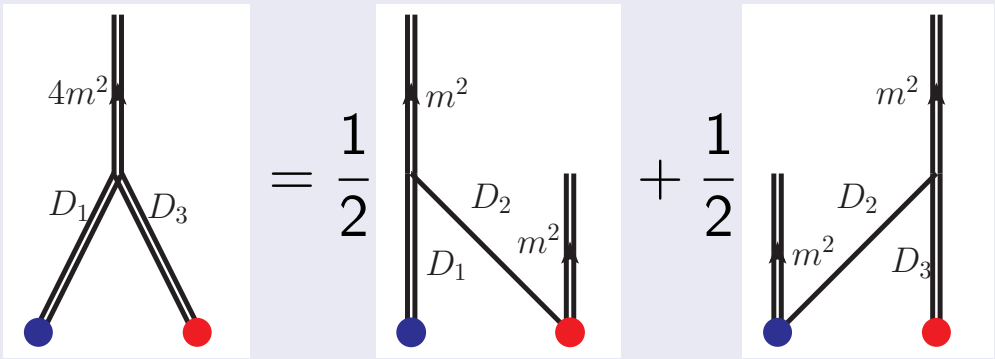

(7)

Partial Fraction Identities

Identity

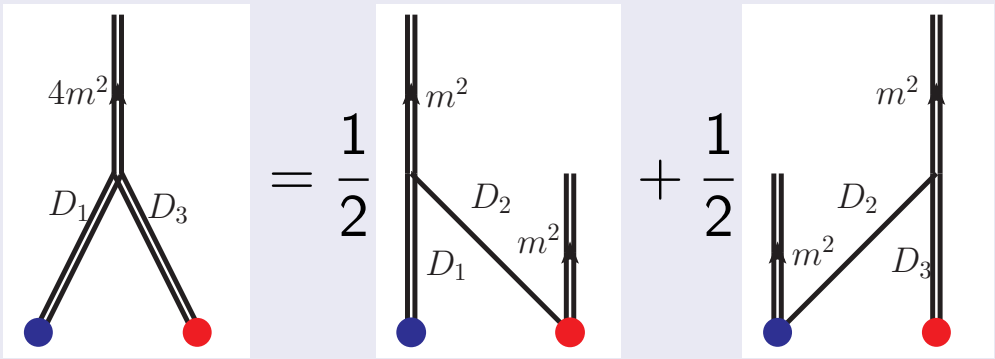

(7)

Example

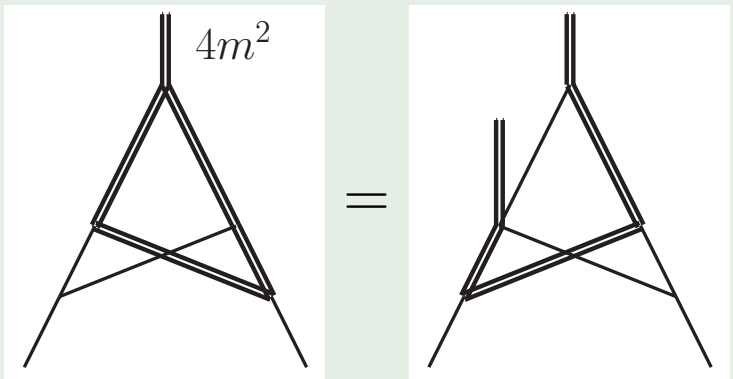

(8)

Triangle Relations

Identity

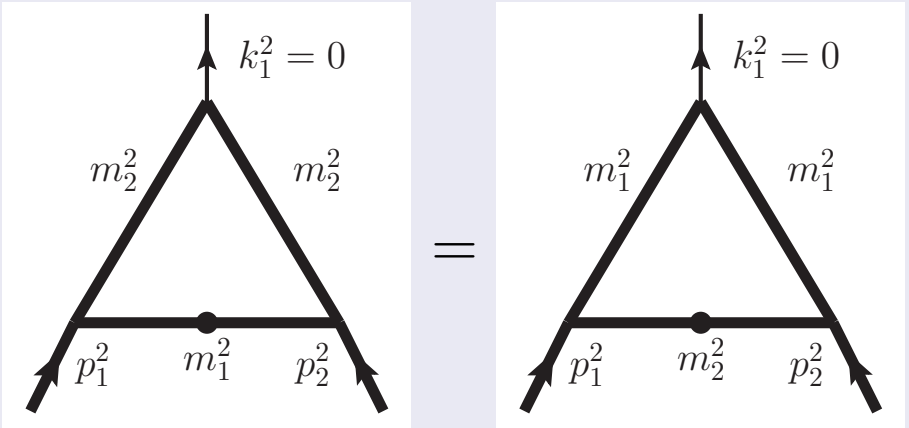

(9)

Triangle Relations

Identity

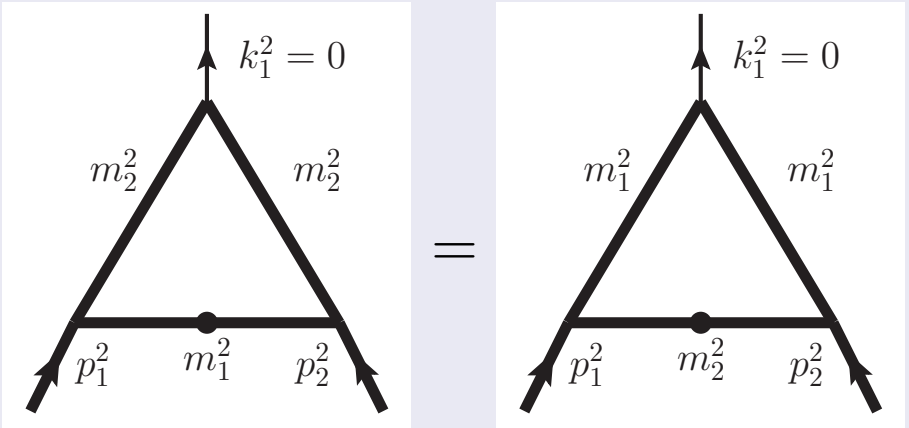

(9)

Example

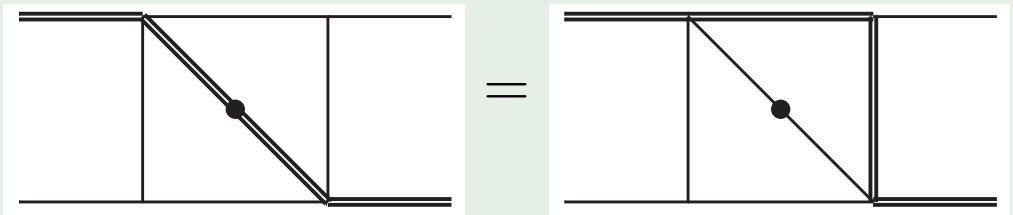

(10)

Topologies and master integrals

- Appearance of 76 master integrals in total
- some are known in general kinematics (see later) but not usable at special kinematics
- Master integrals are seemingly independent, however we find some interesting equivalence relations beyond IBP
  - Partial Fraction Relations
  - Triangle Relations
- Analytical results for most of the integrals in these topologies are not available in the literature

Example: Topology 2

- some topologies would occur also for open $t\bar{t}$-production
- 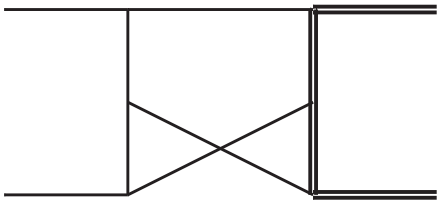

  has been considered for open $t\bar{t}$-production at general kinematics

  [M. Becchetti et al, JHEP 08 (2019) 071]

Example: Topology 2

- some topologies would occur also for open $t\bar{t}$-production
- 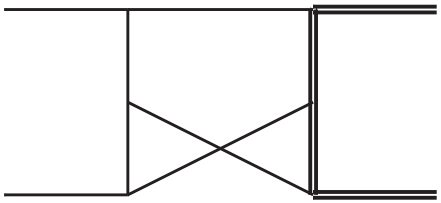

  has been considered for open $t\bar{t}$-production at general kinematics

  [M. Becchetti et al, JHEP 08 (2019) 071]

- However, some prefactors scale as $1/\sqrt{\hat{s} - 4m_Q^2}$

  $\rightarrow$ cannot use analytical results at threshold kinematics $\hat{s} = 4m_Q^2$

Example: Topology 2

- some topologies would occur also for open $t\bar{t}$-production
- 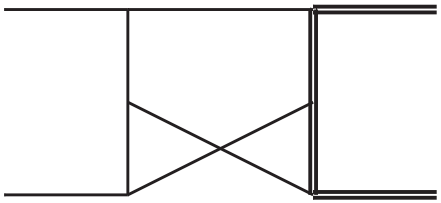

  has been considered for open $t\bar{t}$-production at general kinematics

  [M. Becchetti et al, JHEP 08 (2019) 071]

- However, some prefactors scale as $1/\sqrt{\hat{s} - 4m_Q^2}$

  $\rightarrow$ cannot use analytical results at threshold kinematics $\hat{s} = 4m_Q^2$

- In addition, these prefactors induce a weight drop at $\hat{s} = 4m_Q^2$

  $\rightarrow$ need one order higher in ϵ than available

Example: Topology 2

- some topologies would occur also for open $t\bar{t}$-production
- 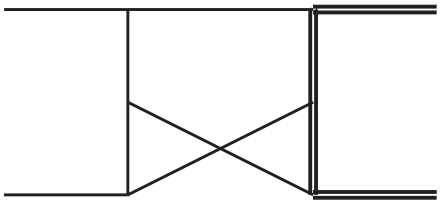

  has been considered for open $t\bar{t}$-production at general kinematics

  [M. Becchetti et al, JHEP 08 (2019) 071]

- However, some prefactors scale as $1/\sqrt{\hat{s} - 4m_Q^2}$

  $\rightarrow$ cannot use analytical results at threshold kinematics $\hat{s} = 4m_Q^2$

- In addition, these prefactors induce a weight drop at $\hat{s} = 4m_Q^2$

  $\rightarrow$ need one order higher in ϵ than available

$\rightarrow$ computed nearly entire topology family via direct integration at threshold

Special functions

- *Multiple Polylogarithms* - points on the *Riemann sphere*
- *elliptic Multiple Polylogarithms* - points on the *torus*
- *iterated integrals of modular forms* - *rational* points on the *torus*

Multiple Polylogarithms (MPLs)

Multiple Polylogarithms (MPLs)

[Goncharov,Remiddi,Vermaseren]

$$G(a_1, ..., a_n; z) = \int_0^z dt \frac{1}{t - a_1} G(a_2, ..., a_n; t) \tag{11}$$

$$G(0; t) = \log t \tag{12}$$

- weight of function corresponds to number of indices $w = n$
- m-loop amplitude usually exhibits functions up to weight of $w = 2m$
  $\rightarrow$ will be useful as cross-check of amplitude
- numerical evaluation can be achieved with `GiNaC`-interface

[Vollinga, Weinzierl]

elliptic Multiple Polylogarithms (eMPLs)

elliptic Multiple Polylogarithms (eMPLs) **[Brown,Levin;Broedel,Duhr,Dulat,Tancredi;Weinzierl...]**

$$E_4\left(\begin{smallmatrix} n_1 \dots n_m \\ c_1 \dots c_m \end{smallmatrix}; x, \vec{q}\right) = \int_0^x dt\, \psi_{n_1}\left(c_1, t, \vec{q}\right) E_4\left(\begin{smallmatrix} n_2 \dots n_m \\ c_2 \dots c_m \end{smallmatrix}; x, \vec{q}\right) \tag{13}$$

$$E_4\left(\begin{smallmatrix} \vec{1} \\ \vec{c} \end{smallmatrix}; x, \vec{q}\right) = G(\vec{c}; x) \tag{14}$$

- $\vec{q}$ are the roots of the elliptic curve defined by

$$y^2 = (x - q_1)(x - q_2)(x - q_3)(x - q_4) \tag{15}$$

- $\psi_{n_1}\left(c_1, t, \vec{q}\right)$ are the elliptic kernels
  - e.g. $\psi_0\left(0, t, \vec{q}\right) = \frac{c_4}{y}$ where $c_4 = \frac{1}{2}\sqrt{(q_1 - q_3)(q_2 - q_4)}$
  - e.g. $\psi_1\left(c, t, \vec{q_r}\right) = \frac{1}{t-c}$
- define weight as $w = \sum_i^m |n_i|$ and length as $l = m$

elliptic Multiple Polylogarithms (eMPLs)

eMPLs in torus representation [Brown,Levin;Broedel,Duhr,Dulat,Tancredi;Weinzierl...]

$$\tilde{\Gamma}\left(\begin{smallmatrix} n_1 \dots n_m \\ z_1 \dots z_m \end{smallmatrix}; z, \tau\right) = \int_0^z dz' \, g^{(n_1)}\left(z' - z_1, \tau\right) \tilde{\Gamma}\left(\begin{smallmatrix} n_2 \dots n_m \\ z_2 \dots z_m \end{smallmatrix}; z', \tau\right) \tag{16}$$

- a torus is double-periodic and can be defined as a two-dimensional lattice

$$\Lambda_\tau = \mathbb{Z} + \mathbb{Z}\tau = \{m + n\tau | m, n \in \mathbb{Z}\} \tag{17}$$

- τ characterises the shape of the torus
- z are the points on the torus within Λ_τ

Iterated integrals of modular forms

if all z_i are rational points on the torus of the form

$$z_i = \frac{r}{N} + \frac{s}{N}\tau \text{ with } 0 \leq r, s < N \text{ and } r, s, N \in \mathbb{N} \tag{18}$$

Iterated integrals of modular forms

if all z_i are rational points on the torus of the form

$$z_i = \frac{r}{N} + \frac{s}{N}\tau \text{ with } 0 \leq r, s < N \text{ and } r, s, N \in \mathbb{N} \tag{18}$$

$\rightarrow$ can rewrite them in terms of iterated integrals of modular forms

$$I(f_1, ..., f_n; \tau) = \int_{i\infty}^{\tau} \frac{d\tau'}{2\pi i} f_1 \, I(f_2, ..., f_n; \tau) \tag{19}$$

$$f_i = h^{(n)}_{N,r,s}(\tau) = - \sum_{\substack{(a,b)\in\mathbb{Z}^2 \\ (a,b)\neq(0,0)}} \frac{e^{2\pi i \frac{(bs-ar)}{N}}}{(a\tau + b)^n} \tag{20}$$

Direct Integration

Feynman integral can be represented via two graph polynomials $\mathcal{U}$ and $\mathcal{F}$ which are the first and second Symanzik polynomial respectively.

$$I = (-1)^a \left(e^{\epsilon\gamma_E}\right)^h \Gamma\left(a - h\frac{D}{2}\right) \int_0^\infty dx_1 \ldots \int_0^\infty dx_m \delta(1-\Delta_H) \times \\ \times \prod_{i=1}^{m} \left(\frac{x_i^{a_i-1}}{\Gamma(a_i)}\right) \frac{\mathcal{U}^{a-(h+1)\frac{D}{2}}}{\mathcal{F}^{a-h\frac{D}{2}}} \tag{21}$$

Direct Integration

Feynman integral can be represented via two graph polynomials $\mathcal{U}$ and $\mathcal{F}$ which are the first and second Symanzik polynomial respectively.

$$I = (-1)^a \left(e^{\epsilon\gamma_E}\right)^h \Gamma\left(a - h\frac{D}{2}\right) \int_0^\infty dx_1 \ldots \int_0^\infty dx_m \delta(1 - \Delta_H) \times \\ \times \prod_{i=1}^{m} \left(\frac{x_i^{a_i - 1}}{\Gamma(a_i)}\right) \frac{\mathcal{U}^{a-(h+1)\frac{D}{2}}}{\mathcal{F}^{a-h\frac{D}{2}}} \tag{21}$$

- each x_i corresponds to a edge/propagator in a graph

Direct Integration

Feynman integral can be represented via two graph polynomials $\mathcal{U}$ and $\mathcal{F}$ which are the first and second Symanzik polynomial respectively.

$$I = (-1)^a \left(e^{\epsilon\gamma_E}\right)^h \Gamma\left(a - h\frac{D}{2}\right) \int_0^\infty dx_1 \ldots \int_0^\infty dx_m \delta(1-\Delta_H) \times \\ \times \prod_{i=1}^{m} \left(\frac{x_i^{a_i-1}}{\Gamma(a_i)}\right) \frac{\mathcal{U}^{a-(h+1)\frac{D}{2}}}{\mathcal{F}^{a-h\frac{D}{2}}} \tag{21}$$

- each x_i corresponds to a edge/propagator in a graph
- the second Symanzik polynomial $\mathcal{F}$ distinguishes between massive and massless propagators
  - each **massless** propagator/edge contributes **linearly** to $\mathcal{F}$
  - each **massive** propagator/edge contributes **quadratically** to $\mathcal{F}$

Direct Integration

Feynman integral can be represented via two graph polynomials $\mathcal{U}$ and $\mathcal{F}$ which are the first and second Symanzik polynomial respectively.

$$I = (-1)^a \left(e^{\epsilon\gamma_E}\right)^h \Gamma\left(a - h\frac{D}{2}\right) \int_0^\infty dx_1 \ldots \int_0^\infty dx_m \delta(1 - \Delta_H) \times \\ \times \prod_{i=1}^{m} \left(\frac{x_i^{a_i - 1}}{\Gamma(a_i)}\right) \frac{\mathcal{U}^{a-(h+1)\frac{D}{2}}}{\mathcal{F}^{a-h\frac{D}{2}}} \tag{21}$$

- each x_i corresponds to a edge/propagator in a graph
- the second Symanzik polynomial $\mathcal{F}$ distinguishes between massive and massless propagators
  - each **massless** propagator/edge contributes **linearly** to $\mathcal{F}$
  - each **massive** propagator/edge contributes **quadratically** to $\mathcal{F}$
- need to integrate out each single edge x_i; one done via Cheng-Wu delta function $\delta(1 - \Delta_H)$.

Direct Integration

We now briefly discuss different cases that we have to consider,

- **linear reducibility**: an order of integration variables can be found where the integration kernels are all linear

Direct Integration

We now briefly discuss different cases that we have to consider,

- **linear reducibility**: an order of integration variables can be found where the integration kernels are all linear

  $\rightarrow$ master integral expressible in terms of *MPLs*

Direct Integration

We now briefly discuss different cases that we have to consider,

- **linear reducibility**: an order of integration variables can be found where the integration kernels are all linear

  $\rightarrow$ master integral expressible in terms of *MPLs*

- **elliptic linear reducibility**: an order of integration variables which is linear reducible excluding the last integration which introduces a square-root

Direct Integration

We now briefly discuss different cases that we have to consider,

- **linear reducibility**: an order of integration variables can be found where the integration kernels are all linear

  $\rightarrow$ master integral expressible in terms of *MPLs*

- **elliptic linear reducibility**: an order of integration variables which is linear reducible excluding the last integration which introduces a square-root

  $\rightarrow$ master integral expressible in terms of *eMPLs*

Direct Integration

We now briefly discuss different cases that we have to consider,

- **linear reducibility**: an order of integration variables can be found where the integration kernels are all linear

  $\rightarrow$ master integral expressible in terms of *MPLs*

- **elliptic linear reducibility**: an order of integration variables which is linear reducible excluding the last integration which introduces a square-root

  $\rightarrow$ master integral expressible in terms of *eMPLs*

- **elliptic next-to-linear reducibility**: an order of integration variables which is linear reducible excluding the second-last integration which introduces a square-root

Direct Integration

We now briefly discuss different cases that we have to consider,

- **linear reducibility**: an order of integration variables can be found where the integration kernels are all linear

  $\rightarrow$ master integral expressible in terms of *MPLs*

- **elliptic linear reducibility**: an order of integration variables which is linear reducible excluding the last integration which introduces a square-root

  $\rightarrow$ master integral expressible in terms of *eMPLs*

- **elliptic next-to-linear reducibility**: an order of integration variables which is linear reducible excluding the second-last integration which introduces a square-root

  $\rightarrow$ requires rationalisation, e.g. `RationalizeRoots`, **[Besier, Wasser, Weinzierl]**

Direct Integration

We now briefly discuss different cases that we have to consider,

- **linear reducibility**: an order of integration variables can be found where the integration kernels are all linear

  $\rightarrow$ master integral expressible in terms of *MPLs*

- **elliptic linear reducibility**: an order of integration variables which is linear reducible excluding the last integration which introduces a square-root

  $\rightarrow$ master integral expressible in terms of *eMPLs*

- **elliptic next-to-linear reducibility**: an order of integration variables which is linear reducible excluding the second-last integration which introduces a square-root

  $\rightarrow$ requires rationalisation, e.g. `RationalizeRoots`, **[Besier, Wasser, Weinzierl]**

  $\rightarrow$ master integral expressible in terms of *eMPLs*

elliptic next-to-linear reducibility & 2nd delta function

The following integral is *elliptic next-to-linear reducible*,

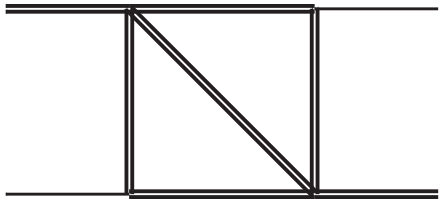

elliptic next-to-linear reducibility & 2nd delta function

The following integral is *elliptic next-to-linear reducible*,

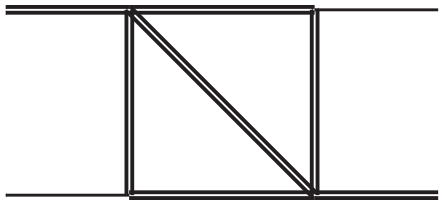

New approach:

elliptic next-to-linear reducibility & 2nd delta function

The following integral is *elliptic next-to-linear reducible*,

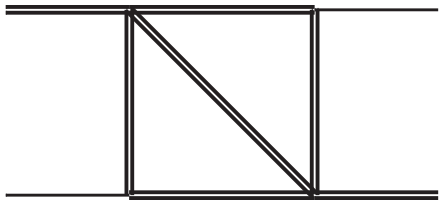

New approach:

- introduce a 2nd delta function similarly to Cheng-Wu delta function, which introduces a new fictitious edge

$$I = (-1)^a \left(e^{\epsilon\gamma_E}\right)^h \Gamma\left(a - h\frac{D}{2}\right) \int_0^\infty dx_1 \ldots \int_0^\infty dx_m \delta(1 - \Delta_H) \times$$
$$\times \int_{-\infty}^{\infty} d\tilde{x}\, \delta\left(1 - \tilde{\Delta}_H\right) \prod_{i=1}^{m} \left(\frac{x_i^{a_i - 1}}{\Gamma(a_i)}\right) \frac{\mathcal{U}^{a-(h+1)\frac{D}{2}}}{\mathcal{F}^{a-h\frac{D}{2}}} \tag{22}$$

elliptic next-to-linear reducibility & 2nd delta function

The following integral is *elliptic next-to-linear reducible*,

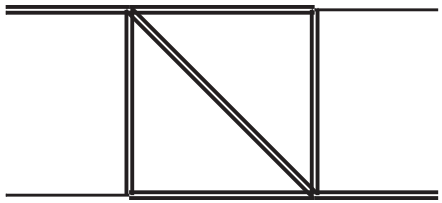

New approach:

- introduce a 2nd delta function similarly to Cheng-Wu delta function, which introduces a new fictitious edge

$$I = (-1)^a \left(e^{\epsilon\gamma_E}\right)^h \Gamma\left(a - h\frac{D}{2}\right) \int_0^\infty dx_1 \ldots \int_0^\infty dx_m \delta(1 - \Delta_H) \times$$
$$\times \int_{-\infty}^{\infty} d\tilde{x}\, \delta\left(1 - \tilde{\Delta}_H\right) \prod_{i=1}^{m} \left(\frac{x_i^{a_i-1}}{\Gamma(a_i)}\right) \frac{\mathcal{U}^{a-(h+1)\frac{D}{2}}}{\mathcal{F}^{a-h\frac{D}{2}}} \tag{22}$$

$\rightarrow$ with suitable choice of $\tilde{\Delta}_H$ can make the integral *elliptic linear reducible* $\rightarrow$ no rationalisation necessary anymore

elliptic next-to-linear reducibility & 2nd delta function

For the following integral

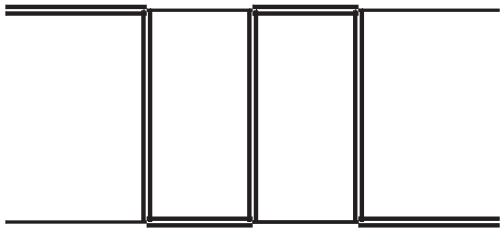

- find coupled roots at second-last integration $\rightarrow$ requires simultaneous rationalisation

elliptic next-to-linear reducibility & 2nd delta function

For the following integral

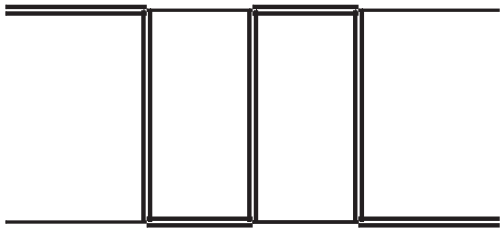

- find coupled roots at second-last integration $\rightarrow$ requires simultaneous rationalisation
- apply new approach with 2nd delta function $\rightarrow$ square-roots are no longer coupled
  $\rightarrow$ can apply *elliptic next-to-linear* reducibility approach

Elliptic Integrals - Last Integration

- For the more difficult integrals encountered, several spurious roots appeared at the last integration, in some cases on order of $\mathcal{O}(20)$ square-roots

Elliptic Integrals - Last Integration

- For the more difficult integrals encountered, several spurious roots appeared at the last integration, in some cases on order of $\mathcal{O}(20)$ square-roots

- coupled square-roots usually beyond scope of eMPLs
  $\rightarrow$ hyper-elliptic structure

Elliptic Integrals - Last Integration

- For the more difficult integrals encountered, several spurious roots appeared at the last integration, in some cases on order of $\mathcal{O}(20)$ square-roots

- coupled square-roots usually beyond scope of eMPLs
  $\rightarrow$ hyper-elliptic structure

- however, can eliminate all spurious roots using a systematic and algorithmic approach

Elliptic Integrals - Last Integration

- For the more difficult integrals encountered, several spurious roots appeared at the last integration, in some cases on order of $\mathcal{O}(20)$ square-roots
- coupled square-roots usually beyond scope of eMPLs
  $\rightarrow$ hyper-elliptic structure
- however, can eliminate all spurious roots using a systematic and algorithmic approach
- classify and fibrate terms in integrand according to different criteria

Elliptic Integrals - Last Integration

- For the more difficult integrals encountered, several spurious roots appeared at the last integration, in some cases on order of $\mathcal{O}(20)$ square-roots
- coupled square-roots usually beyond scope of eMPLs
  $\rightarrow$ hyper-elliptic structure
- however, can eliminate all spurious roots using a systematic and algorithmic approach
- classify and fibrate terms in integrand according to different criteria
  - **weight** of functions

Elliptic Integrals - Last Integration

- For the more difficult integrals encountered, several spurious roots appeared at the last integration, in some cases on order of $\mathcal{O}(20)$ square-roots

- coupled square-roots usually beyond scope of eMPLs
  $\rightarrow$ hyper-elliptic structure

- however, can eliminate all spurious roots using a systematic and algorithmic approach

- classify and fibrate terms in integrand according to different criteria
  - **weight** of functions
  - **prefactors** depending on integration variable

Elliptic Integrals - Last Integration

- For the more difficult integrals encountered, several spurious roots appeared at the last integration, in some cases on order of $\mathcal{O}(20)$ square-roots

- coupled square-roots usually beyond scope of eMPLs
  $\rightarrow$ hyper-elliptic structure

- however, can eliminate all spurious roots using a systematic and algorithmic approach

- classify and fibrate terms in integrand according to different criteria
  - **weight** of functions
  - **prefactors** depending on integration variable

- all spurious roots disappear one by one and we are left with a single elliptic curve $\rightarrow$ eMPLs

Master Integrals - Elliptic Curves

We encounter two different types of elliptic curves,

- one is associated to the elliptic sunrise

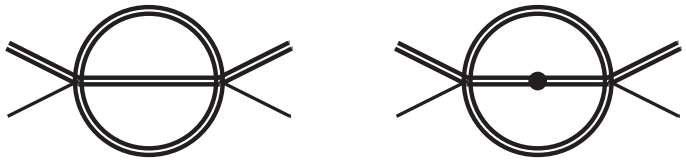

$$\vec{q} = \left(\frac{1}{2}\left(1-\sqrt{1+2i}\right), \frac{1}{2}\left(1-\sqrt{1-2i}\right), \frac{1}{2}\left(1+\sqrt{1+2i}\right), \frac{1}{2}\left(1+\sqrt{1-2i}\right)\right) \tag{23}$$

- the other is associated to the master integral

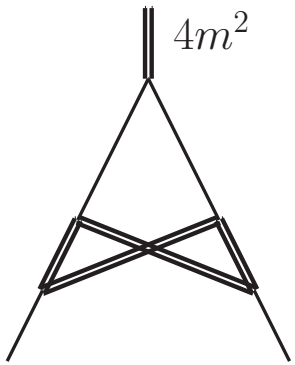

$$\vec{q} = \left(1-\sqrt{5}, 0, 2, 1+\sqrt{5}\right) \tag{24}$$

and appears only in light-by-light scattering contribution

Analytics and Numerics

- computed all integrals **analytically** via direct integration

Analytics and Numerics

- computed all integrals **analytically** via direct integration
  - class 1: MPL integrals
    $\rightarrow$ high-precision numerics with `GiNaC`-package

Analytics and Numerics

- computed all integrals **analytically** via direct integration
  - class 1: MPL integrals
    $\rightarrow$ high-precision numerics with `GiNaC`-package
  - class 2: iterated integrals of modular forms
    $\rightarrow$ high-precision numerics with algorithm **[Duhr, Tancredi, JHEP 02 (2020) 105]**

Analytics and Numerics

- computed all integrals **analytically** via direct integration
  - class 1: MPL integrals
    $\rightarrow$ high-precision numerics with `GiNaC`-package
  - class 2: iterated integrals of modular forms
    $\rightarrow$ high-precision numerics with algorithm **[Duhr, Tancredi, JHEP 02 (2020) 105]**
  - class 3: eMPLs integrals
    $\rightarrow$ numerics: convergence is rather slow, make use of differential equation approach and solve numerically via series expansion approach, e.g. `DiffExp` **[Hidding, arXiv:2006.05510]**

Analytics and Numerics

- computed all integrals **analytically** via direct integration
  - class 1: MPL integrals
    $\rightarrow$ high-precision numerics with `GiNaC`-package
  - class 2: iterated integrals of modular forms
    $\rightarrow$ high-precision numerics with algorithm **[Duhr, Tancredi, JHEP 02 (2020) 105]**
  - class 3: eMPLs integrals
    $\rightarrow$ numerics: convergence is rather slow, make use of differential equation approach and solve numerically via series expansion approach, e.g. `DiffExp` **[Hidding, arXiv:2006.05510]**

$\rightarrow$ produced high-precision numerics (200 digits)

Analytics and Numerics

- computed all integrals **analytically** via direct integration
  - class 1: MPL integrals
    $\rightarrow$ high-precision numerics with `GiNaC`-package
  - class 2: iterated integrals of modular forms
    $\rightarrow$ high-precision numerics with algorithm **[Duhr, Tancredi, JHEP 02 (2020) 105]**
  - class 3: eMPLs integrals
    $\rightarrow$ numerics: convergence is rather slow, make use of differential equation approach and solve numerically via series expansion approach, e.g. `DiffExp` **[Hidding, arXiv:2006.05510]**

  $\rightarrow$ produced high-precision numerics (200 digits)

- validation of results numerically with `pySecDec` (only few digits)

Analytics and Numerics

- computed all integrals **analytically** via direct integration
  - class 1: MPL integrals
    $\rightarrow$ high-precision numerics with `GiNaC`-package
  - class 2: iterated integrals of modular forms
    $\rightarrow$ high-precision numerics with algorithm **[Duhr, Tancredi, JHEP 02 (2020) 105]**
  - class 3: eMPLs integrals
    $\rightarrow$ numerics: convergence is rather slow, make use of differential equation approach and solve numerically via series expansion approach, e.g. `DiffExp` **[Hidding, arXiv:2006.05510]**

  $\rightarrow$ produced high-precision numerics (200 digits)
- validation of results numerically with `pySecDec` (only few digits)
- PSLQ procedure: find additional relations between elliptic integrals beyond equivalence relations shown before

Form-factors

Now ready to plug in analytics and numerics for the form-factors.
Validation of results,

Form-factors

Now ready to plug in analytics and numerics for the form-factors.
Validation of results,

- compare to known numerical results for $\gamma\gamma \leftrightarrow \eta_Q$ case
  $\rightarrow$ find full agreement **[A. Czarnecki, K. Melnikov, Phys.Lett.B 519 (2001) 212-218]** **[F. Feng, Y. Jia, W.-L. Sang, Phys.Rev.Lett. 115 (2015) 22, 222001]**

Form-factors

Now ready to plug in analytics and numerics for the form-factors.
Validation of results,

- compare to known numerical results for $\gamma\gamma \leftrightarrow \eta_Q$ case
  $\rightarrow$ find full agreement **[A. Czarnecki, K. Melnikov, Phys.Lett.B 519 (2001) 212-218]** **[F. Feng, Y. Jia, W.-L. Sang, Phys.Rev.Lett. 115 (2015) 22, 222001]**

- for the new form-factors, validation is based on universal IR pole structure $\rightarrow$ amplitudes are manifestly finite after UV and IR renormalisation **[Catani; Becher, Neubert]**

Form-factors

Now ready to plug in analytics and numerics for the form-factors.
Validation of results,

- compare to known numerical results for $\gamma\gamma \leftrightarrow \eta_Q$ case
  $\rightarrow$ find full agreement **[A. Czarnecki, K. Melnikov, Phys.Lett.B 519 (2001) 212-218]** **[F. Feng, Y. Jia, W.-L. Sang, Phys.Rev.Lett. 115 (2015) 22, 222001]**
- for the new form-factors, validation is based on universal IR pole structure $\rightarrow$ amplitudes are manifestly finite after UV and IR renormalisation **[Catani; Becher, Neubert]**
- all amplitudes contain functions of maximal weight $w = 4$ (e.g. π^4, $\log^4 2$, $\pi\zeta_3$).

Form-factors

Now ready to plug in analytics and numerics for the form-factors.
Validation of results,

- compare to known numerical results for $\gamma\gamma \leftrightarrow \eta_Q$ case
  $\rightarrow$ find full agreement **[A. Czarnecki, K. Melnikov, Phys.Lett.B 519 (2001) 212-218]** **[F. Feng, Y. Jia, W.-L. Sang, Phys.Rev.Lett. 115 (2015) 22, 222001]**
- for the new form-factors, validation is based on universal IR pole structure $\rightarrow$ amplitudes are manifestly finite after UV and IR renormalisation **[Catani; Becher, Neubert]**
- all amplitudes contain functions of maximal weight $w = 4$ (e.g. π^4, $\log^4 2$, $\pi\zeta_3$).
- regular Abelian corrections $\left(C_F^2, C_F T_F n_{h/l}\right)$ are identical for all form-factors $\rightarrow$ further confirmation of the new form-factor results

Form-factors

Now ready to plug in analytics and numerics for the form-factors.
Validation of results,

- compare to known numerical results for $\gamma\gamma \leftrightarrow \eta_Q$ case
  $\rightarrow$ find full agreement **[A. Czarnecki, K. Melnikov, Phys.Lett.B 519 (2001) 212-218]** **[F. Feng, Y. Jia, W.-L. Sang, Phys.Rev.Lett. 115 (2015) 22, 222001]**
- for the new form-factors, validation is based on universal IR pole structure $\rightarrow$ amplitudes are manifestly finite after UV and IR renormalisation **[Catani; Becher, Neubert]**
- all amplitudes contain functions of maximal weight $w = 4$ (e.g. π^4, $\log^4 2$, $\pi\zeta_3$).
- regular Abelian corrections $\left(C_F^2, C_F T_F n_{h/l}\right)$ are identical for all form-factors $\rightarrow$ further confirmation of the new form-factor results
- QED corrections to para-Positronium result, agreement with existing numerical results in literature **[A. Czarnecki, K. Melnikov, A. Yelkhovsky, Phys.Rev.A 61 (2000) 052502]**

Part III

Decay of para-Positronium to di-photon at NNLO accuracy

para-Positronium decay width to di-photon

The decay width of para-Positronium to di-photon can be expressed as

$$\Gamma_{\text{p-Ps}\to\gamma\gamma} = \Gamma_0 \left[1 + \left(\frac{\alpha_{em}}{\pi}\right) K_1 + 2\alpha_{em}^2 \log\frac{1}{\alpha_{em}} + \left(\frac{\alpha_{em}}{\pi}\right)^2 K_2 - \frac{3\alpha_{em}^3}{2\pi}\log^2\frac{1}{\alpha_{em}} + \frac{\alpha_{em}^3}{\pi} C_2 \log\frac{1}{\alpha_{em}} + \mathcal{O}\left(\alpha_{em}^3\right)\right] \tag{25}$$

para-Positronium decay width to di-photon

The decay width of para-Positronium to di-photon can be expressed as

$$\Gamma_{\text{p-Ps}\to\gamma\gamma} = \Gamma_0 \left[1 + \left(\frac{\alpha_{em}}{\pi}\right) K_1 + 2\alpha_{em}^2 \log\frac{1}{\alpha_{em}} + \left(\frac{\alpha_{em}}{\pi}\right)^2 K_2 - \frac{3\alpha_{em}^3}{2\pi}\log^2\frac{1}{\alpha_{em}} + \frac{\alpha_{em}^3}{\pi} C_2 \log\frac{1}{\alpha_{em}} + \mathcal{O}\left(\alpha_{em}^3\right)\right] \tag{25}$$

- we computed two-loop coefficient K_2 analytically and have numerics up to 200 digits accuracy

para-Positronium decay width to di-photon

The decay width of para-Positronium to di-photon can be expressed as

$$\Gamma_{\text{p-Ps}\to\gamma\gamma} = \Gamma_0 \left[1 + \left(\frac{\alpha_{em}}{\pi}\right) K_1 + 2\alpha_{em}^2 \log\frac{1}{\alpha_{em}} + \left(\frac{\alpha_{em}}{\pi}\right)^2 K_2 - \frac{3\alpha_{em}^3}{2\pi}\log^2\frac{1}{\alpha_{em}} + \frac{\alpha_{em}^3}{\pi} C_2 \log\frac{1}{\alpha_{em}} + \mathcal{O}\left(\alpha_{em}^3\right)\right] \tag{25}$$

- we computed two-loop coefficient K_2 analytically and have numerics up to 200 digits accuracy
  $\to$ in a position to provide ultra-precise predictions for total decay width (2γ, 4γ)

para-Positronium decay width to di-photon

The decay width of para-Positronium to di-photon can be expressed as

$$\Gamma_{\text{p-Ps}\to\gamma\gamma} = \Gamma_0 \left[1 + \left(\frac{\alpha_{em}}{\pi}\right) K_1 + 2\alpha_{em}^2 \log\frac{1}{\alpha_{em}} + \left(\frac{\alpha_{em}}{\pi}\right)^2 K_2 - \frac{3\alpha_{em}^3}{2\pi}\log^2\frac{1}{\alpha_{em}} + \frac{\alpha_{em}^3}{\pi} C_2 \log\frac{1}{\alpha_{em}} + \mathcal{O}\left(\alpha_{em}^3\right)\right] \tag{25}$$

- we computed two-loop coefficient K_2 analytically and have numerics up to 200 digits accuracy
  $\to$ in a position to provide ultra-precise predictions for total decay width (2γ, 4γ)

$$\Gamma^{\text{theory, NNLO}}_{\text{p-Ps decay}} = 7989.618221(4)\,(\mu s)^{-1} \tag{26}$$

para-Positronium decay width to di-photon

The decay width of para-Positronium to di-photon can be expressed as

$$\Gamma_{\text{p-Ps}\to\gamma\gamma} = \Gamma_0 \left[1 + \left(\frac{\alpha_{em}}{\pi}\right) K_1 + 2\alpha_{em}^2 \log\frac{1}{\alpha_{em}} + \left(\frac{\alpha_{em}}{\pi}\right)^2 K_2 - \frac{3\alpha_{em}^3}{2\pi}\log^2\frac{1}{\alpha_{em}} + \frac{\alpha_{em}^3}{\pi} C_2 \log\frac{1}{\alpha_{em}} + \mathcal{O}\left(\alpha_{em}^3\right)\right] \tag{25}$$

- we computed two-loop coefficient K_2 analytically and have numerics up to 200 digits accuracy
  $\to$ in a position to provide ultra-precise predictions for total decay width (2γ, 4γ)

$$\Gamma^{\text{theory, NNLO}}_{\text{p-Ps decay}} = 7989.618221(4)\,(\mu s)^{-1} \tag{26}$$

$$\Gamma^{\text{exp.}}_{\text{p-Ps decay}} = 7990.9(1.7)\,(\mu s)^{-1} \tag{27}$$

para-Positronium decay width to di-photon

The decay width of para-Positronium to di-photon can be expressed as

$$\Gamma_{\text{p-Ps}\to\gamma\gamma} = \Gamma_0 \left[1 + \left(\frac{\alpha_{em}}{\pi}\right) K_1 + 2\alpha_{em}^2 \log\frac{1}{\alpha_{em}} + \left(\frac{\alpha_{em}}{\pi}\right)^2 K_2 - \frac{3\alpha_{em}^3}{2\pi}\log^2\frac{1}{\alpha_{em}} + \frac{\alpha_{em}^3}{\pi} C_2 \log\frac{1}{\alpha_{em}} + \mathcal{O}\left(\alpha_{em}^3\right)\right] \tag{25}$$

- we computed two-loop coefficient K_2 analytically and have numerics up to 200 digits accuracy
  $\to$ in a position to provide ultra-precise predictions for total decay width (2γ, 4γ)

$$\Gamma^{\text{theory, NNLO}}_{\text{p-Ps decay}} = 7989.618221(4)\,(\mu s)^{-1} \tag{26}$$

$$\Gamma^{\text{exp.}}_{\text{p-Ps decay}} = 7990.9(1.7)\,(\mu s)^{-1} \tag{27}$$

  $\to$ experimental precision studies in future, e.g. J-PET

Summary

- computed all two-loop master integrals **analytically**
- produced high-precision numerics (200 digits)
- find some interesting equivalence relations
- have complete **analytical** results for form-factors available
- form-factors are finite after UV and IR renormalisation

  $\rightarrow$ ready for phenomenological applications

Thank you for attention!

Backup

Direct Integration

linear reducibility: an order of integration variables can be found where the integration kernels are all linear

- for each integration can fibrate integrand into canonical form using MPL kernels only

  $\rightarrow$ master integral expressible in terms of MPL functions

- algorithmic approach implemented e.g. `HyperInt`, `PolyLogTools`, but in some cases need to perform integration manually

- 54 MIs expressible in terms of MPL functions
  - 50 MIs expressible in terms of MPLs with indices at 6th root of unity
  - 4 MIs involve indices beyond 6th root of unity, e.g. Catalan constant

Direct Integration

elliptic linear reducibility: an order of integration variables where all integration kernels excluding the last integration are linear und contains a square-root in the last integration.

- for all integrations excluding the last integration can fibrate the integrand into canonical form using MPL kernels only
- for last integration, appearance of elliptic curve $y \rightarrow$ need to use eMPL kernels

  $\rightarrow$ master integral expressible in terms of eMPL functions

- in principle algorithmic apart from some technicalities but quite tedious and computational heavy

- 17 MIs in this class and expressible in terms of eMPL functions

Direct Integration

elliptic next-to-linear reducibility: an order where all integration kernels up and excluding the second-last integration are linear. The second-last integration contains a square-root.

- for all integrations up and excluding the second-last integration can fibrate the integrand into canonical form using MPL kernels only
- for second-last integration have quadratic variable $\rightarrow$ need to rationalise square-root with e.g. `RationalizeRoots`, **[Besier, Wasser, Weinzierl]**

  $\rightarrow$ perform second-last integration with MPL kernels
- for last integration have appearance of elliptic curve y $\rightarrow$ need to use eMPL kernels

  $\rightarrow$ master integral expressible in terms of eMPL functions
- 5 MIs in this class but with some additional obstacles...

Exclusive decay width to di-photon

- variation of scales
  - three scales in quarkonium physics: mv^2, mv, m
  - $\mu_{\text{NRQCD}} = mv$, ($v^2 = 0.3$ for charmonium, $v^2 = 0.1$ for bottomonium)
  - central: $\mu_R = M = 2m$, variation: $\mu_R \in \left[M/\sqrt{2}, \sqrt{2}M\right]$

  Charmonium:

$$\Gamma^{\text{NLO}}_{\eta_c \to \gamma\gamma} = \Gamma_0 \times \left[0.737^{+0.032}_{-0.044}\right] = \left(10.34^{+0.45}_{-0.62}\right) \text{keV} \tag{28}$$

$$\boxed{\Gamma^{\text{NNLO}}_{\eta_c \to \gamma\gamma} = \Gamma_0 \times \left[0.28^{+0.11}_{-0.17}\right] = \left(3.9^{+1.6}_{-2.3}\right) \text{keV}} \tag{29}$$

- μ_R uncertainty has contrary to expectation not reduced from NLO to NNLO
- latest experimental data [Particle Data Group]

$$\Gamma^{\text{exp}}_{\eta_c \to \gamma\gamma} = (5.06 \pm 0.34)\,\text{keV} \tag{30}$$

- NNLO result is closer to experimental value than NLO result $\rightarrow$ importance of higher order corrections

Exclusive decay width to di-photon

- variation of scales
  - three scales in quarkonium physics: mv^2, mv, m
  - $\mu_{\rm NRQCD} = mv$, ($v^2 = 0.3$ for charmonium, $v^2 = 0.1$ for bottomonium)
  - central: $\mu_{\rm R} = M = 2m$, variation: $\mu_{\rm R} \in \left[M/\sqrt{2}, \sqrt{2}M\right]$

  Bottomonium:

$$\Gamma^{\rm NLO}_{\eta_b\to\gamma\gamma} = \Gamma_0 \times \left[0.809^{+0.016}_{-0.019}\right] = \left(3.977^{+0.077}_{-0.093}\right) \text{ keV} \tag{31}$$

$$\boxed{\Gamma^{\rm NNLO}_{\eta_b\to\gamma\gamma} = \Gamma_0 \times \left[0.724^{+0.016}_{-0.018}\right] = \left(3.560^{+0.078}_{-0.087}\right) \text{ keV}} \tag{32}$$

- $\mu_{\rm R}$ uncertainty is almost same for NLO and NNLO
- no experimental data available in [Particle Data Group]
- NNLO are important